

# Efficient Digital Hologram Generation using Position Clustering and FFT-based Structural Modification

ChoongSang Cho<sup>1</sup> and Sangkeun Lee<sup>\*, 2</sup>

<sup>1</sup> Korea Electronics Technology Institute / Seongnam, Korea

<sup>2</sup> Chung-Ang University ./ Seoul, Korea

\*Corresponding Author (sangkny@cau.ac.kr)

**Abstract:** In a digital hologram, 3D information of an object is recorded on a holographic fringe pattern obtained from the interference pattern between the object and reference waves, or the numerical diffraction equations. Numerical equation-based hologram generation is highly computationally complex because the relationship between a point of the object and all the positions on a fringe pattern need to be considered. In this work, we present an efficient method for digital hologram generation using position clustering and FFT-based structural modification by Taylor series approximation. To evaluate the performance of the proposed method, it was compared to the Rayleigh-Sommerfeld (RS) diffraction for two point clouds and the gray and depth images were used to generate a digital hologram. Experimental results show that the proposed method has much lower computational complexity in terms of the numerical structure while similar visual quality was preserved; the proposed method is adjudged to more suitable for parallel processing. Therefore, we believe that the proposed method can be a useful tool for numerical digital hologram generation.

**Keywords:** Fast Hologram Generation, Image based Hologram Generation.

Received Jun. 15, 2016; accepted for publication Nov. 03, 2016; published online Nov. 30, 2016. DOI: 10.15323/techart.2016.08.3.4.35 / ISSN: 2288-9248.

## 1. Introduction

Recently, digital holography has become an important technique because it can provide three-dimensional information corresponding to a real object [1]. In a digital hologram, 3D information of an object is recorded on a holographic fringe pattern obtained by the interference pattern between the object and reference waves, or the numerical diffraction equations [2]-[6]. The basic diffraction equation is obtained by finding a solution of the Helmholtz equation for a propagating wave encountering a partially obscured planar screen [4]-[6]. Rayleigh-Sommerfeld (RS) diffraction, which is widely used for digital hologram generation, is obtained by imposing a boundary condition on a diffracting screen [4]-[6]. In generating the hologram, the Point Light Source (PLS)-based approach for modeling a 3D object is widely used because of the simple and useful structure for parallel processing. To compute the fringe pattern using the numerical diffraction equation, diffraction patterns of all PLSs are accumulated. However, numerically calculating the wavefronts of all PLSs has high computational complexity, because the relationship between a point on the object and all positions of a fringe pattern has to be considered [7]. Therefore, to reduce the complexity and computational time required to generate the numerical digital hologram, several approaches have been suggested. In [7], the circular symmetry of a zone plate is used to

reduce the complexity by using a look-up-table (LUT) for the zone plate. A single line having complex amplitude for a zone plate is calculated along the radial axis, and the line is rolled to form a complete zone plate. However, this approach requires memory space for the LUT, and its performance is heavily dependent on the ability to draw a discrete circle. For a pre-calculated interference pattern, LUT-based methods have been proposed to reduce the complexity and the LUT memory space [8]-[10]. These methods effectively reduce the complexity, but their performance strongly depends on the accuracy of the LUT, and requires pre-calculation and memory space for the LUT. Hardware-based methods, including field-programmable gate arrays (FPGA) and graphics processing units (GPU) have been employed to reduce the computational time for fringe pattern generation [10]. When using these methods, the processing time is much faster than a method that only uses the central processing unit (CPU). However, their performance is dependent on the characteristics of the type of processor used, and includes the additional cost of the hardware. In this work, an efficient method for digital hologram generation is presented based on clustering point clouds according to the z-axis and FFT-based structural modification using Taylor series approximation. The proposed method is explained numerically, and its practical procedure is described experimentally in Section 2. Experimental results are compared with state-of-the-art algorithms in Section 3, followed by summarizing and concluding the given algorithm with some discussion.

## 1. Proposed Method: Fast and Flexible Digital Hologram Generation

A basic diffraction equation is obtained by finding a solution of the Helmholtz equation for a propagating wave encountering a partially obscured planar screen [2]–[6]. The Rayleigh-Sommerfeld (RS) solution, which is widely employed for generating digital holograms, is computed by imposing a boundary condition for the case where a diffracting screen is placed in the  $z = 0$  plane [4]. To generate the fringe pattern for a 3D object that can be represented as a point cloud, diffraction patterns of all points are accumulated as [4]

$$\Gamma(\xi, \eta) = -\frac{i}{\lambda} \int_{-\infty}^{\infty} \int_{-\infty}^{\infty} \int_{-\infty}^{\infty} A(x, y, z) \frac{\exp(ik\rho)}{\rho} \cos[\chi(x, y, z)] dx dy dz$$

$$\rho = \sqrt{(\xi - x)^2 + (\eta - y)^2 + (d - z)^2} \quad (1)$$

where  $k = 2\pi/\lambda$ ,  $(\xi, \eta)$ , and  $(x, y, z)$  are the coordinates for the fringe pattern and a 3D object, respectively.  $d$  is the focal length of generating the digital hologram,  $\lambda$  is a wavelength.  $A(x, y, z)$  and  $\chi$  are the point amplitude and the diffraction angle at  $(x, y, z)$ , respectively;  $\rho$  indicates the distance between a point in the object and a point in the fringe pattern. For simplification, the diffraction angle at each point is assumed to be zero, and Eq.1 is approximated [9] by

$$\Gamma(\xi, \eta) = \frac{-i}{\lambda d} \int_{-\infty}^{\infty} \int_{-\infty}^{\infty} \int_{-\infty}^{\infty} A(x, y, z) \exp\left(i \frac{2\pi}{\lambda} \rho\right) dx dy dz \quad (2)$$

The distance  $\rho$  can be expressed by

$$\rho = \sqrt{(\xi - x)^2 + (\eta - y)^2 + (d - z)^2}$$

$$= \sqrt{d^2 \left[ 1 + \frac{(x - \xi)^2 + (y - \eta)^2 + z^2 - 2dz}{d^2} \right]}$$

$$= d \sqrt{1 + \frac{(x - \xi)^2 + (y - \eta)^2 + z^2 - 2dz}{d^2}} \quad (3)$$

The distance is converted to the distance  $\rho'$  using the first order Taylor series expansion as

$$\rho' = d \left\{ 1 + \frac{1}{2} \left[ \frac{(x - \xi)^2 + (y - \eta)^2 + z^2 - 2dz}{d^2} \right] \right\}$$

$$= d + \frac{1}{2} \left[ \frac{(x - \xi)^2 + (y - \eta)^2 + z^2 - 2dz}{d} \right] \quad (4)$$

The difference between the focused and defocused diffraction angle of the points, which are affected by the distance, is reduced by the distance approximation. The range of the focused and defocused diffraction angles

becomes narrow, and many points of a 3D object have a similar focused and defocused diffraction angle.

To compensate for the reduction in diffraction angle after the distance approximation, the focusing distance  $d$  is controlled by a symmetrical kernel function with the  $z$ -axis as

$$d' = d \times f(\xi, \eta),$$

$$f(\xi, \eta) = 1 + \text{sign}[z_p(\xi, \eta)] \times K \frac{\exp\left(\frac{1}{N/2} z_p(\xi, \eta)\right) - 1}{\exp(1) - 1}$$

, and  $z_p(\xi, \eta) = z \times N/2$  (5)

where  $K$  is a weighting factor,  $N$  is the  $z$ -axis dimension of a point cloud, and the range of the normalized  $z$  is  $[-1; 1]$ .

By applying the approximated distance  $\rho'$  and the controlled focusing length  $d'$ , the numerical digital hologram generation is rewritten by

$$\Gamma'(\xi, \eta) = \frac{-i}{\lambda d'} \int_{-\infty}^{\infty} \int_{-\infty}^{\infty} \int_{-\infty}^{\infty} A(x, y, z) \exp\left(i \frac{2\pi}{\lambda} D(x, y, z)\right) dx dy dz$$

$$D(x, y, z) = \left\{ d' + \frac{1}{2} \left[ \frac{(x - \xi)^2 + (y - \eta)^2 + z^2 - 2zd'}{d'} \right] \right\} \quad (6)$$

To induce its mathematical similarity with the Fourier Transform, it can be expressed as

$$\Gamma'(\xi, \eta) = \int_{-\infty}^{\infty} \int_{-\infty}^{\infty} \int_{-\infty}^{\infty} W(\xi, \eta) P(x, y, z) \exp\left\{-i \frac{\pi}{\lambda d'} [2(x\xi + y\eta)]\right\} dx dy dz$$

$$\equiv \frac{-i}{\lambda d'} \exp\left(i \frac{2\pi}{\lambda} d'\right) \exp\left[i \frac{\pi}{\lambda d'} (\xi^2 + \eta^2)\right] P(x, y, z)$$

$$\equiv A(x, y, z) \exp\left\{i \frac{\pi}{\lambda d} [(x^2 + y^2 + z^2 - 2zd')]\right\} \quad (7)$$

Next, two variables  $\nu$  and  $\mu$  are employed as

$$\nu = \frac{\xi}{\lambda d'} \quad \text{and} \quad \mu = \frac{\eta}{\lambda d'} \quad (8)$$

and Eq. 8 is substituted into Eq. 7, and then the approximated generation is formulated in the form of a Fast Fourier Transform (FFT) as

$$\Gamma(\xi, \eta) \approx \Gamma'(\xi, \eta) = \int_{-\infty}^{\infty} W(\xi, \eta) \text{FFT}\{aM(x, y, z, d')\} dz$$

$$aM(x, y, z, d') = A(x, y, z) \exp\left[i \frac{\pi}{\lambda d'} (x^2 + y^2 + z^2 - 2dz)\right] \quad (9)$$

To transform the continuous form in Eq.9 to a discrete form [5], [11], the coordinates for the fringe pattern and a 3D object are converted into discrete terms as

$$\xi = m\Delta\nu, \eta = n\Delta\mu, x = k\Delta x, y = l\Delta y, z = j\Delta z$$

$$\Delta\nu = \frac{1}{N\Delta x}, \Delta\mu = \frac{1}{M\Delta y}, \Delta\xi = \frac{\lambda d'}{N\Delta x}, \Delta\eta = \frac{\lambda d'}{M\Delta y} \quad (10)$$

where  $N$  and  $M$  are the discrete point number of  $x$  and  $y$  in the fringe pattern, respectively.  $\Delta x$ ,  $\Delta y$ , and  $\Delta z$  are the result of the discretization step of  $x$ ,  $y$  and  $z$ -axis of a 3D object position, respectively.

By substituting Eq. 10 into Eq. 9, the discrete equation for the approximated fast generation is obtained by

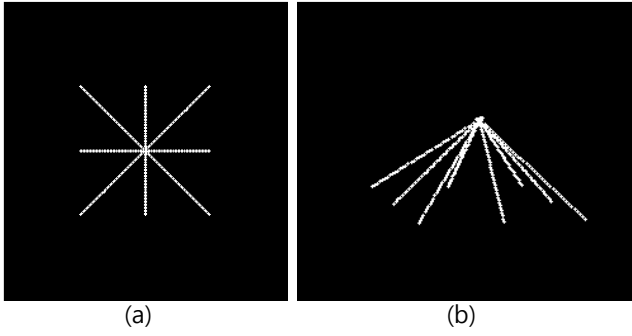


Fig 1. Points cloud for a radial shape to generate a fringe pattern, (a) front view of points cloud; and (b) side view of points cloud.

$$\Gamma'_d(m, n) = \sum_{j=0}^{J-1} (W(m, n) FFT \{dM(k, l, j)\})$$

$$dM(k, l, j) = A(k, l, j) \exp \left[ i \frac{\pi}{\lambda d'} (k^2 \Delta x^2 + l^2 \Delta y^2 + j^2 \Delta z^2 - 2d'j \Delta z) \right] \quad (11)$$

where  $J$  is the number of position clusters according to the focusing distance  $\Delta z$ .

In Eq.11, the points having the same discrete  $z$ -axis position are calculated using an FFT, and the corresponding result is weighted by  $W(m, n)$ . Each result for a different discrete  $z$ -axis position is independently calculated and accumulated. In the approximated discrete generation process, the complexity is determined by the numbers of grouped  $z$ -axis positions, and is flexibly controlled by the quantization step size  $\Delta z$  in the  $z$ -axis.

### 3. Experiment

For the performance evaluation, the proposed method is compared to the previous method using two point clouds and evaluated using the gray and depth images.

As shown in Fig.1, the first cloud consisting of 321 points for a radial shape is designed to show that the defocused diffraction angle gradually increases according to the distance from the focused center point to the  $z$  position. The normalized  $z$  position has a zero value at the focused center point, and the  $z$  position increases to 0.4 by 0.01. In addition, the 1361 point cloud for a car is used to verify if the proposed method is suitable for a general point cloud. Two fringe patterns with  $1024 \times 1024$  pixel resolution were generated by applying the 321 point cloud to both the Rayleigh-Sommerfeld (RS) diffraction and the proposed method, as illustrated in Figs. 2 (a) and (b). The patterns were then reconstructed using the Fresnel approximation with a wavelength  $\lambda = 633 \text{ nm}$  and a pixel pitch  $\Delta = 15.2 \mu\text{m}$ , as illustrated in Figs. 2 (c) and (d).

For better observation, the center and side regions were magnified four times their actual size as insets. In the RS diffraction, the reconstructed points in the center region are focused, while the points in the side region are gradually defocused as the distance increases from the focused center.

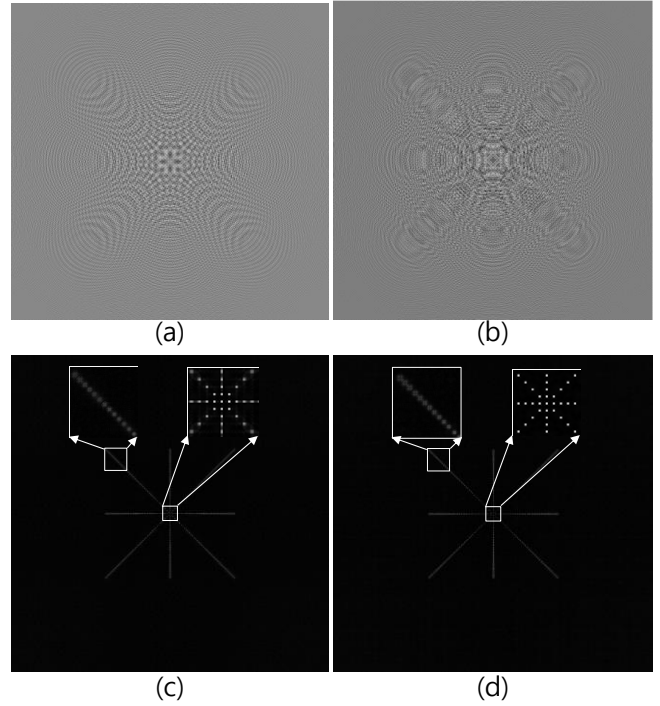


Fig. 2. Generated fringe pattern and reconstructed results for each algorithm; (a) fringe pattern by RS diffraction; (b) fringe pattern by the proposed method; (c) reconstructed result of (a); and (d) reconstructed result of (b).

Similarly, in the proposed method, both the focused and defocused regions are gradually obtained in the center and side regions as shown in Fig. 2(d). The gradually defocused patterns of the RS diffraction result are similar to the pattern of the proposed method. In a similar manner, the fringe patterns with a  $1024 \times 1024$  pixel resolution were generated by applying the 1361 point cloud to both the RS diffraction and the proposed method, as illustrated in Figs. 3(a) and (b). The patterns were then reconstructed using the Fresnel approximation with a wavelength  $\lambda = 633 \text{ nm}$  and a pixel pitch  $\Delta = 15.2 \mu\text{m}$ , as shown in Fig. 3(c) and (d).

The focused and defocused regions were enlarged twice their actual size as insets. In the enlarged images, the focused and defocused regions of the two methods are similar to each other and the defocused diffraction angle of the proposed method increases from the front to the rear part of the car like the RS diffraction method.

To compare the complexity of each algorithm, a point cloud consisting of  $C$  points is used and assumed to have  $g$  numbers along the  $z$  axis. In other words, the  $z$  axis is divided into  $g$  groups by the quantization step  $\Delta z$ . Because the size of the fringe pattern is  $N \times N$ , the RS diffraction method requires  $C \times N \times N$  square root, and  $C \times N \times N$  multiplication and addition. On the other hand, the proposed method requires  $g \times (N \times N) \log(N \times N)$

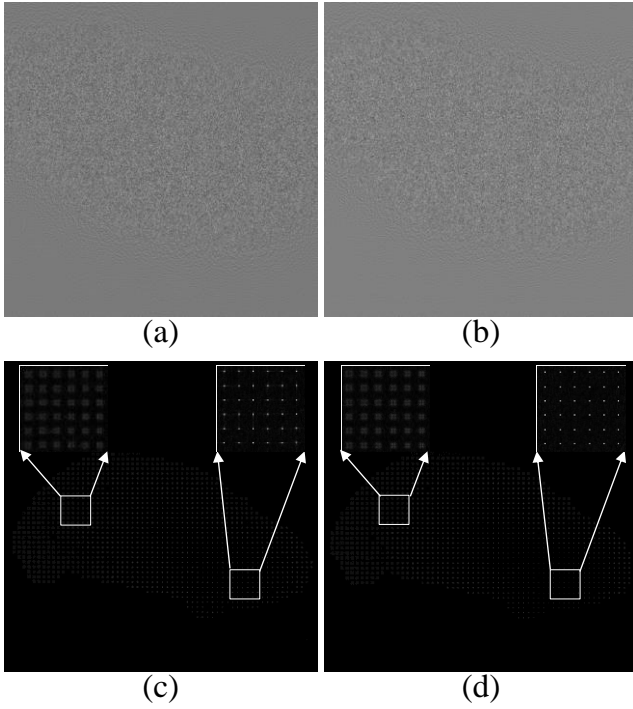


Fig. 3. Generated fringe pattern and reconstructed results for each algorithm; (a) fringe pattern by RS diffraction; (b) fringe pattern by the proposed scheme; (c) reconstructed result of (a); and (d) reconstructed result of (b).

for FFT, and  $g \times (N \times N)$  multiplication and addition without the square root operation. The complexity of the proposed method depends on the number of  $z$ -axis data types, and can be flexibly controlled by changing the quantization step  $\Delta z$ . By using a rough quantization step, or creating large clusters of similar  $z$ -axis data, the number of  $z$ -axis groups can be decreased, thereby reducing the complexity involved in the generation of a hologram. However, the resolution of the focused and defocused diffraction angle is decreased. It is noted that the complexity of the proposed method depends heavily on the complexity of the FFT. Fortunately, several low-complexity FFT methods have been proposed [12], [13] and are applicable to the proposed method.

To evaluate the performance of the image, the gray and depth images with  $2560 \times 1920$  resolution, are used for the amplitude and distance, respectively, to generate the digital hologram, as shown in Figs. 4(a) and (b). The image contains about 5 million pixels and is considered a PLS for the digital hologram generation. Using the proposed method, the fringe pattern was obtained as shown in Fig. 3(c). The pattern then was reconstructed using the Fresnel approximation with a wavelength  $\lambda = 633 \text{ nm}$  and a pixel pitch  $\Delta = 15.2 \mu\text{m}$  as shown in Fig. (d).

To evaluate the computational complexity for sequential processing, we implemented the proposed method for sequential processing in ANSI-C on a machine with an Intel Core i7-3960 3.3 GHz CPU with 28 GB of RAM. The

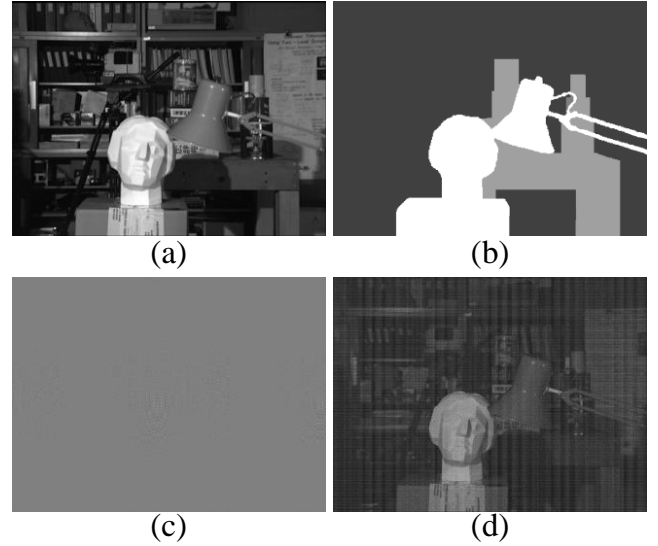


Fig. 4. Generated fringe pattern and reconstructed results of the gray and depth images; (a) gray image; (b) depth image; (c) fringe pattern; and (d) reconstructed result of (c).

computational time of the proposed method was measured at 3.89 seconds.

## 4. Conclusion

A simple and effective method for numerical digital hologram generation was proposed by clustering the similar  $z$ -axis data and FFT-based structural modification by Taylor series approximation. In particular, the Taylor series was used to calculate the approximated distance between a point in the object and a point in the fringe pattern, and a symmetrical kernel function was adapted for the controllable focusing distance. In addition, the numerical approximation result in the FFT-based digital hologram generation equation reduced the computational complexity. To evaluate the proposed method, two point clouds for a radial shape and a car were used to generate the fringe pattern using RS diffraction and the proposed method. The patterns were then reconstructed using the Fresnel approximation. Experimental results showed that the proposed method could allow the defocused diffraction angle to increase according to the distance from the focused point. In addition, a shape and pattern were obtained from the reconstructed results of the fringe patterns that were similar to the RS diffraction method. In terms of complexity, the proposed method has a dependency on the number of  $z$ -axis data types, so the complexity and quality of the numerical generation can be controlled by manipulating the quantization step size.

In addition, the performance of the proposed method was evaluated by using the gray and depth image ( $2560 \times 1920$  pixels); it took 3.89 seconds to generate the digital hologram. The proposed method was found to have much lower computational complexity when compared to the method in the numerical structure. Moreover, it is more

suitable for parallel processing while preserving similar visual quality of the conventional approach.

Therefore, we believe that the proposed method can be a useful tool for numerical digital hologram generation.

## Acknowledgements

This work was partially supported by the Basic Science Research Program through the National Research Foundation of Korea (NRF) funded by the Ministry of Education, Science and Technology (2013-029824), by the Commercializations Promotion Agency for R&D Outcomes (COMPA)(No.2016K000202), by the Korean Government (MSIP) (No. NRF-2014R1A2A1A11049986), and by [GK130100, Development of Interactive and Realistic Massive Giga-Content Technology]

## References

- [1] L. Onural, F. Yaras, and H. Kang, "Digital holographic three-dimensional video displays," *Proc. IEEE*, vol.99, no.4, pp. 576-589, 2011.
- [2] C. Cho, B. Choi, H. Kang, and S. Lee, "Numerical twin image suppression by nonlinear segmentation mask in digital holography," *Opt. Express*, vol. 20, no. 20, pp. 22454-22464, 2013.
- [3] C. Cho, B. Choi, H. Kang, and S. Lee, "Laplace Operation-Based DC Noise Reduction in Digital Holography," *IEEE Photon. Tech. Letters*, vol.25, no. 12, pp. 1188-1191, 2013.
- [4] R. L. Lucke, "Rayleigh-Sommerfeld diffraction and Poisson's spot," *Euro. Jour. of Physic*, vol. 27, no. 2, pp. 193-204, 2006.
- [5] U. Schnars and W.P.Juptner, "Digital recording and numerical reconstruction of hologram," *Meas. Sci. Technol.*, vol.13, no. 9, pp. 85-101, 2002.
- [6] J. W. Goodman, *Introduction to Fourier Optics*, Roberts & Company, 2004.
- [7] T. Shimobaba, T. Kakue, N. Masuda, and T. Ito, "Fast calculation of computer-generated hologram using the circular symmetry of zone plates," *Opt. Express*, vol.20, no. 25, pp. 27496-27502, 2012.
- [8] S. C. Kim and E. S. Kim, "Effective generation of digital holograms of three-dimensional objects using a novel look-up table method," *Appl. Opt.*, vol.47, no. 19, pp. 55-62, 2008.
- [9] S. C. Kim, J. M. Kim, and E. S. Kim, "Effective memory reduction of the novel look-up table with one-dimensional sub-principle fringe pattern in computer-generated holograms," *Opt. Express*, vol. 20, no. 18, pp. 12021-12034, 2012.
- [10] T. Shimobaba, T. Ito, N. Masuda, Y. Ichihashi, and N. Takada, "Fast calculation of computer-generated-hologram on AMD HD5000 series GPU and OpenCL," *Opt. Express*, vol. 18, no. 10, pp. 9955-9960, 2010.
- [11] U. Schnars and W. P. Juptner, "Digital Holography: Digital Hologram Recording, Numerical Reconstruction, and Related Techniques," Springer, 2005.
- [12] M Frigo and S. G. Johnson, "The design and implementation of FFTW3," *Proc. IEEE*, vol. 93, no.2, pp. 216-231, 2005.
- [13] NVIDIA, *CUFFT Library User's Guide* (<http://docs.nvidia.com/cuda/cufft/>,2013).

## Biographies



**Choongsang Cho** received his B.S. degree in electronics engineering from Suwon University, Gyeonggi, Korea, in 2006. He received his M.S. degree from the Department of Information and Communications, Gwangju Institute of Science and Technology, Gwangju, Korea, in 2008, and his Ph.D. degree in Graduate School of Advanced Imaging Science, Multimedia and Film, Chung-Ang University, Seoul, Korea, in 2016. Since 2008, he has been a Researcher with the Multimedia IP Research Center, Korea Electronics Technology Institute, Gyeonggi. His research interests include image enhancement and segmentation, and digital holograms.



**Sangkeun Lee** received his B.S. and M.S. degrees in electronics engineering from Chung-Ang University, Seoul, Korea, in 1996 and 1999, respectively, and his Ph.D. degree in electrical and computer engineering from the Georgia Institute of Technology, Atlanta, GA, in 2003. From 2003 to 2008, he was a Staff Research Engineer with the Digital Media Solutions Laboratory, Samsung Information Systems America, Irvine, CA, USA, where he was involved in the development of video processing and enhancement algorithms for Samsung's HDTV. He is currently an Associate Professor with the Graduate School of Advanced Imaging Science, Multimedia and Film, Chung-Ang University. His current research and development interests include digital video and image processing, vision computing, especially video analysis/synthesis, denoising, compression for UHD TV, and multimedia applications, as well as CMOS image sensors.